Int J Legal Med (2005) 119: 355–362
DOI 10.1007/s00414-005-0541-0

ORIGINAL ARTICLE

M. Bohnert · R. Walther · T. Roths · J. Honerkamp

A Monte Carlo-based model for steady-state diffuse reflectance spectrometry in human skin: estimation of carbon monoxide concentration in livor mortis

Received: 15 October 2004 / Accepted: 23 March 2005 / Published online: 21 April 2005

Abstract In terms of physics, the skin can be regarded as an optically turbid medium in which the light is mainly scattered by the collagen fibers, mitochondria and cell nuclei, whereas the absorption is determined by the content of reduced hemoglobin, oxyhemoglobin, bilirubin, and melanin. When the measuring geometry and the illumination spectrum are known, the optical characteristics of the skin can be approximately described by the diffusion and absorption coefficients. These values define the diffusion and absorption probability per unit distance traveled for each wavelength. Based on these parameters, a mathematical skin model was developed with the help of Monte Carlo simulations. By implementing the absorption coefficient of carbon monoxide hemoglobin (CO-Hb) into the skin model, the authors wanted to investigate whether this method is suitable to determine the CO-Hb concentration from spectral reflectance curves of livores. The investigations performed on 28 deaths from CO poisoning so far showed that this is generally possible. In almost all cases, the actual CO-Hb values could be estimated correctly by using the Monte Carlo simulations.

Keywords Monte Carlo simulation · Livores · Carbon monoxide hemoglobin · Reflectance spectrometry

Introduction

Repeated attempts have been made to characterize postmortem phenomena of corpse skin by means of optical methods [4–7, 9–11, 21, 24, 25, 31–35, 44–46, 48, 51, 52]. Special attention was devoted to providing an objective way to determine the chronological order of the occurrence of livores and their intensity and displaceability [24, 25, 32, 45, 46, 51, 52]. The color quality of livores was less often investigated [9, 32, 45].

Under low ambient temperatures, livor mortis may adopt a bright red, pink, or cherry red color due to the resaturation of hemoglobin with oxygen. The most important differential diagnosis in the presence of pink hypostasis is carbon monoxide (CO) poisoning. Safe diagnosis of CO intoxication based on the subjective impression of the color alone is seldom possible within the scope of the postmortem examination, in particular if the CO-hemoglobin (CO-Hb) values are relatively low. Previous investigations have shown that it is not possible to distinguish between exposure to a cold environment and CO poisoning if the color of livor mortis is objectively determined by colorimetric methods [9]. However, these investigations also proved that at high concentrations of CO-Hb there is a characteristic shift of the reflectance maxima and flattening of the spectral reflectance curves, which allows a distinction in these cases [9].

Generally one may assume that there is also a functional relationship between the spectral reflectance of the skin and its optical properties or components. The question was whether it is possible to develop a mathematical skin model simulating the optical behavior of the skin and to estimate the CO-Hb concentration from the reflectance spectra of hypostasis with this model.

Optical properties of human skin

The human skin represents a very complex organ with a three-layered structure consisting of the stratum corneum, stratum germinativum, and dermis. The thin stratum corneum causes regular reflectance at the tissue–air transition. This regular reflectance is due to the refractive index mismatch of the stratum corneum ($n_{sc}\approx1.55$) and air ($n_{air}=1.0$). In the visible light range, skin reflects between 4 and 7% of the incident beam, nearly independent of wavelength and

M. Bohnert (✉)
Institute of Legal Medicine, Albert Ludwig University,
Albertstrasse 9,
79104 Freiburg, Germany
e-mail: michael.bohnert@uniklinik-freiburg.de
Tel.: +49-761-2036854
Fax: +49-761-2036858

R. Walther · T. Roths · J. Honerkamp
Freiburg Material Research Center, Albert Ludwig University,
Stefan-Meier-Strasse 21,
79104 Freiburg, Germany

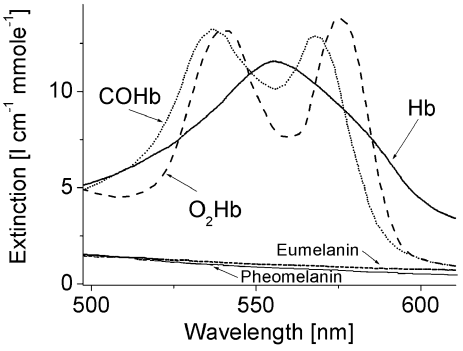

Fig. 1 Extinction spectra of the main absorbers of human skin in the visible wave range [1, 40, 47]

skin type [1]. The stratum germinativum and dermis are composed of many organelles and substructures that influence the transport of light. However, the main scattering processes are elastic scattering processes by collagen fibers and mitochondria. In a good approximation, the collagen fibers and mitochondria can be described by a spherical scatterer with a diameter d between 0.1 and 0.8 μm and a refractive index n_{cf} of 1.4. The surrounding medium has a refractive index n_{cp} of 1.36 [13, 41, 55]. In the visible range of light, the absorption processes are mainly due to hemoglobin and melanin [1]. The respective extinction spectra are shown in Fig. 1. In a first approximation the human skin can be modeled as a turbid, absorbing, semi-infinite medium composed of homogeneously distributed scatterers and absorbers.

Light transport in turbid media

If a collimated incident pencil beam is directed at the surface of the turbid medium, part of the light is reflected at the air–medium interface due to the refractive index mismatch. The photons, which pass through the surface and enter the turbid medium, undergo many scattering processes in their path. In every scattering process, the photon changes its direction randomly, and thus the light transport represents a stochastic process, i.e., a random walk. This process can be described by three probabilities: (1) the probability for a scattering process per length scale, which is given by the scattering coefficient μ_s; (2) the probability for an absorption process per length scale, which is given by the absorption coefficient μ_a; and (3) the phase function $p(\cos\theta)$, which describes the probability for the cosine of the scattering angle θ for a single scattering process. To achieve a simple, workable model, the phase function $p(\cos\theta)$ is often parameterized based on the anisotropy factor g which represents the first momentum of the phase function. These optical parameters depend on the wavelength of the incident light, the size and refractive index of the particles and concentration of the absorber in the medium. Therefore, the modeling of the light transport in turbid absorbing media can be divided into two parts: (1) the description of the light transport based on the optical parameters μ_s, μ_a, and g and (2) the modeling of these optical parameters based on microscopic parameters such as size and density of the scattering particles and absorber concentrations.

Light transport in turbid media can be described by the Boltzmann transport equation [22, 50]. However, because of its complexity this integral equation is not very suitable for data analysis of reflectance spectra. A very useful simplification of the Boltzmann transport equation is the diffusion approximation [22, 50]. This approach for the description of light transport in turbid media has the disadvantage of not being valid near strong light sources and for a large amount of absorption. Thus, unfortunately the diffusion approximation is not very well suited for modeling the reflectance spectrum of human skin around an incident light beam [2, 53]. An alternative approach for the description of light transport in turbid absorbing media is given by Monte Carlo simulations, which are not restricted to large distances from strong sources and a small amount of absorption [26, 54]. Thus, we have used such Monte Carlo

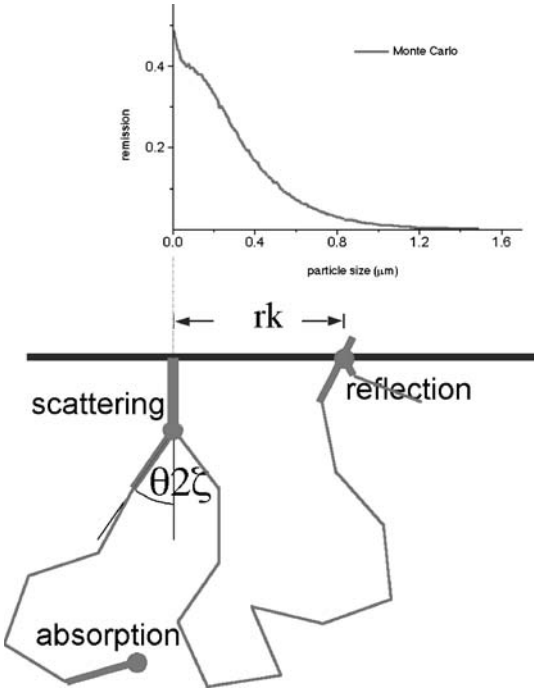

Fig. 2 Monte Carlo simulation of photon migration in turbid absorbing media. The graphic illustrates the interactions between the photon package and the turbid medium: scattering, absorption, reflection, and transmission at the surface. If the photon package is transmitted, e.g., at a distance r from the incident pencil beam, the current size of the photon package contributes to the reflectance of the surface. Thus, the reflectance of the concerning circlet $R_{circlet}(r)=2\pi r d_r R(r)$ with radius r and thickness d_r (depending on the discretization of r) is increased by the value of the photon package size. The resulting reflectance of the circlets around the incident pencil beam divided by 2π is shown above the surface of the medium

simulations to establish a numerical model for the measured reflectance spectrum based on the optical parameters μ_s, μ_a, and g.

Monte Carlo simulation

The Monte Carlo simulation is a widely used method for the analysis of very complex or stochastic systems. To estimate the diffuse reflectance $R(\mu_s, \mu_a, g)$ at the skin surface, the underlying stochastic process within the skin, i.e., the random walk of the photons, is realized very often. The principles of Monte Carlo simulations for the description of light transport in turbid media are described in detail in the literature [26, 54]. For our investigations, we adapted a Monte Carlo algorithm by Wang et al. [54]. The algorithm is described briefly in the following (Fig. 2).

First, a so-called photon package is initialized. It is much more efficient and comfortable to simulate many photons at once in such a photon package than to simulate single photon paths. Thus, a photon package with a weight of w=1 is placed at the origin of a coordinate system on the surface of the turbid medium with a certain direction $\vec{s}$ (often, this direction $\vec{s}$ is chosen to be normal to the surface of the medium, but other directions can also be initialized easily). Then, this photon package is moved in direction $\vec{s}$ with a step size of Δs. The step size is calculated by means of a uniformly distributed random number, in the following denoted as $\zeta \in (0,1)$, according to

$$\Delta s = -\frac{\ln \xi}{\mu_s + \mu_a},$$

so that it represents a random number with a probability density of

$$p(\Delta s) = (\mu_s + \mu_a) e^{-(\mu_s+\mu_a)\Delta s},$$

which gives the probability of a photon–medium interaction per path length. The random number ζ has to be determined for each random variable Δs, φ, and θ in every iteration step.

Then, the absorption along this path is considered by reducing the size of the photon package w according to

$$w \leftarrow w \left(1 - \frac{\mu_a}{\mu_s + \mu_a}\right).$$

Now, the new direction of the photon package is calculated. The scattering angle of the scattering process is calculated by use of the phase function $p(\cos\theta)$, which is approximated by the Henyey–Greenstein function [20, 49]. Thus, the realization of the cosine of the scattering angle can be calculated according to

$$\cos\theta = \begin{cases} \frac{1}{2g}\left[1 + g^2 - \left(\frac{1-g^2}{1-g+2g\zeta}\right)^2\right] & g > 0 \\ 2\zeta - 1 & g = 0 \end{cases}.$$

The azimuth angle is uniformly distributed and can be calculated by

$$\phi = 2\pi\zeta.$$

The step size Δs is calculated again and the photon package is moved along the new direction specified by θ and φ. When the photon package hits a boundary, the Fresnel formula

$$R_{\text{Fresnel}}(\theta) \begin{cases} \frac{1}{2}\left[\left(\frac{n_2\cos\theta' - n_1\cos\theta}{n_2\cos\theta' + n_1\cos\theta}\right)^2 + \left(\frac{n_2\cos\theta - n_1\cos\theta'}{n_2\cos\theta + n_1\cos\theta'}\right)^2\right] & 0 < \theta < \theta_c \\ 1 & \theta_c < \theta < \pi/2 \end{cases}$$

is used to calculate the probability of a reflection at the boundary. Here, n_1 and n_2 are the refractive indices of the surroundings (e.g., air) and the medium (e.g., cytoplasm); θ' denotes the reflection angle of the photon package, which is obtained by solving the law of refraction

$$n_1 \sin\theta\prime = n_2 \sin\theta.$$

Again, a uniformly distributed random number $\zeta \in (0,1)$ is used in order to make the decision of reflection and transmission at the boundary: for random numbers

$$\zeta < R_{\text{Fresnel}}(\theta)$$

reflection occurs. Otherwise, the photon package is transmitted at the boundary. Then the size of the photon package is added to the respective reflectance $R(\rho)$ at the surface and another photon package is launched. Here ρ denotes the radial distance from the incident pencil beam. If reflection occurs, the direction $\vec{s}$ of the photon package is changed by inverting the sign of the z component of the direction $\vec{s}$. Then, the photon package is moved for the remaining step size and another scattering iteration starts. The run of a photon package ends if it is transmitted at the surface or it is terminated by the "roulette method" [19]. This method terminates the run of very small photon packages in an un-

biased way. To generate Monte Carlo simulation for different optical properties with the same or even comparable accuracy the heuristic formula for the number of photon packages $N(\mu_s, \mu_a)$ is very useful [27]:

$$N(\mu_s, \mu_a) = \left(\frac{\mu_a}{\mu_s}\right)^{1/4} \times 10^6.$$

One simulation for a certain set of optical parameters requires, on an Intel Celeron, 1.7 GHz, up to 3 h, so the whole simulation, consisting of up to 1,000 simulations (depending on the discretization of μ_s, μ_a, and g), takes several weeks. However, these simulations for different optical properties can be calculated parallely on different PCs to speed up the effective simulation time. Furthermore, these simulations have to be calculated only once while the experimental setup is not changed; thus, this large effort occurs only once.

The Monte Carlo simulation described above leads to realizations of the spatially resolved reflectance $R(\rho|\mu_s, \mu_a, g)$ at a distance ρ from the incident pencil beam at the surface of a diffuse medium based on the optical parameters μ_s, μ_a, and g. To calculate the reflectance R_{r_c} measured at a collection area around the incident pencil beam, the spatial resolved reflectance $R(\rho|\mu_s, \mu_a, g)$ has to be integrated numerically over the collection area with radius r_c:

$$R_{r_c}(\mu_s, \mu_a, g) = \int_0^{2\pi} \mathrm{d}\phi \int_0^{r_c} \rho \, \mathrm{d}\rho \, R(\rho|\mu_s, \mu_a, g),$$

Finally, mapping of the measured reflectance $R_{r_c}(\mu_s, \mu_a, g)$ on the optical parameters μ^s, μ^a, and g is established. This mapping is very smooth and can be interpolated easily, e.g., by means of spline function or neuronal nets, for further processing. All the reflectance and the optical parameters depend on wavelength. Thus, parameterization of the optical parameters is required.

The calculation of the reflectance $R_{r_c}(\mu_s, \mu_a, g)$ described above implies a cylindric symmetry or, in other words, a perpendicular incident light beam. Nevertheless, the Monte Carlo simulations can also be calculated for non-perpendicular incident light beams and the emitted photon packages from an arbitrary area can be counted. However, such simulations have two disadvantages. First, the simulation run time increases rapidly because many photon packages are needed to yield a sufficient accuracy (two dimensions instead of one). Second, this approach is less flexible in terms of changing the diameter of the probe. Using the approach described above, one can establish a "database" of Monte Carlo simulation results and, for different probe diameters, the reflectance can be calculated very easily and fast.

Modeling of the optical parameters μ_s, μ_a, and g

The scattering coefficient μ_s denotes the probability of a scattering event per unit length. Thus, it can be written as

$$\mu_s(\lambda) = N C_{scat}(d, \lambda),$$

where N denotes the particle concentration, i.e., the number of particles per unit volume, and C_{scat} is the scattering cross section. For polydispersed particles with particle size distribution $h(d)$ Eq. (2) reads

$$\mu_s(\lambda) = \int_{d_{min}}^{d_{max}} h(d) C_{scat}(d, \lambda) \mathrm{d}d.$$

Assuming spherical particles, the scattering cross section C_{scat} and the anisotropy factor $g(d,\lambda)$ can be obtained using the Mie theory in dependence of particle size and wavelength [55]. For given extinction spectra $\varepsilon_i(\lambda)$ of M absorber in the medium the absorption coefficient can be written as

$$\mu_a(c, \lambda) = \ln 10 \sum_{i=1}^{M} c_i \, \varepsilon_i(\lambda),$$

where c_i denotes the concentration of the ith absorber. The factor ln 10 arises from the conversion from extinction to absorption probability per length scale. For the investigations presented in this article, oxy- (O_2-Hb) and desoxyhemoglobin (Hb), carbon monoxide hemoglobin (CO-Hb), eumelanin, and pheomelanin are considered as main absorbers (Fig. 1).

Combining Eq. 1 with Eqs. 3 and 4, the "direct problem," i.e., the mapping of the measured reflectance in dependence of the particle size distribution $h(d)$ of the scatterer and the absorber concentrations c_i of O_2-Hb, Hb, and CO-Hb and the skin pigments eumelanin and pheomelanin, is established. The desired parameters $h(d)$ and c_i can now be estimated by inversion of the direct problem.

Inverse problem

In this article we focus on the estimation of the CO-Hb concentration in livores. There is no need of a high resolution of the particle size distribution of the light scattering in human skin. Therefore, the direct problem can be inverted by means of a least squares fit as described below. Otherwise, if one is interested in a highly resolved particle size distribution, special mathematical methods, e.g., regularization methods, are required to estimate the particle distribution [20, 49].

To estimate the concentration of oxy-, desoxy-, and carbon monoxide hemoglobin (c_{Hb}, c_{O_2Hb}, c_{COHb}, respectively)—and the particle size distribution $h(d)$ in a low resolution d_1,..., d_N, N=8, and the eumelanin c_{eu} and pheomelanin c_{pheo}—from a measured reflectance spectrum $R^{\sigma}(\lambda_i)$, $i = 1, \ldots, M$ the inverse problem was solved by minimizing the discrepancy

$$D(h_{1,\ldots,N}, c_{Hb}, c_{O_2Hb}, c_{COHb}, c_{eu}, c_{pheo}) = \frac{1}{M}\sum_{i=1}^{M}\left\{R^{s}(\lambda_i) - R\left[\mu_s(h_{1,\ldots,N}|\lambda_i), \mu_a\left(c_{Hb}, c_{O_2Hb}, c_{COHb}, c_{eu}, c_{pheo}|\lambda_i\right), g\left(h_{1,\ldots,N}|\lambda_i\right)\right]\right\}^2$$

by means of a Levenberg–Marquardt algorithm [42]. M denotes the number of measured data points of the reflectance spectrum.

Depending on the discretization, various difficulties by the minimization occur. As mentioned above, for a highly resolved particle size distribution the inverse problem becomes ill posed and a regularization method has to be used (e.g., Tikhonov–Philips regularization, singular value decomposition) [20, 49]. For low resolutions of the particle size distribution the inverse problem turns into a well-posed inverse problem and standard fitting routines (e.g., Newton, Levenberg–Marquardt, Powell) can be used. If the particle size d and the number h of the particles with size d are to be estimated, large correlations between particle size d and number of particles h complicates the minimization. To overcome this difficulty and to avoid sticking to a local minimum different starting values for d and h have to be chosen. In addition, the concentration of eumelanin and pheomelanin show correlations if the desired range of wavelength is very small, e.g., 500–600 nm. However, these correlations do not influence the estimation of the concentration of oxy-, desoxy-, and carbon monoxide hemoglobin.

Materials and methods

Study material

Spectrophotometric studies of hypostasis were performed on 32 Caucasian bodies undergoing forensic autopsy for suspected carbon monoxide poisoning. The study included 20 men and 12 women, ages 2 to 88 years (mean, 44 years). The postmortem interval was up to 4 days; the bodies were stored at 4–6°C until examination. No external signs of putrefaction were visible. Burned bodies were excluded from the study. CO-Hb levels were determined by spectrophotometric analysis of heart blood [15] obtained during autopsy and ranged between 2 and 79%.

Investigation method

Measurements were performed with a diode array spectrophotometer MCS 400 (Carl-Zeiss-Jena GmbH, Jena, Germany) with a halogen bulb as light source (standard illuminant D65). The measuring head allowed recording of the directed surface reflection of a 5-mm-wide measuring spot (measuring geometry 45°/45°). Compressed barium

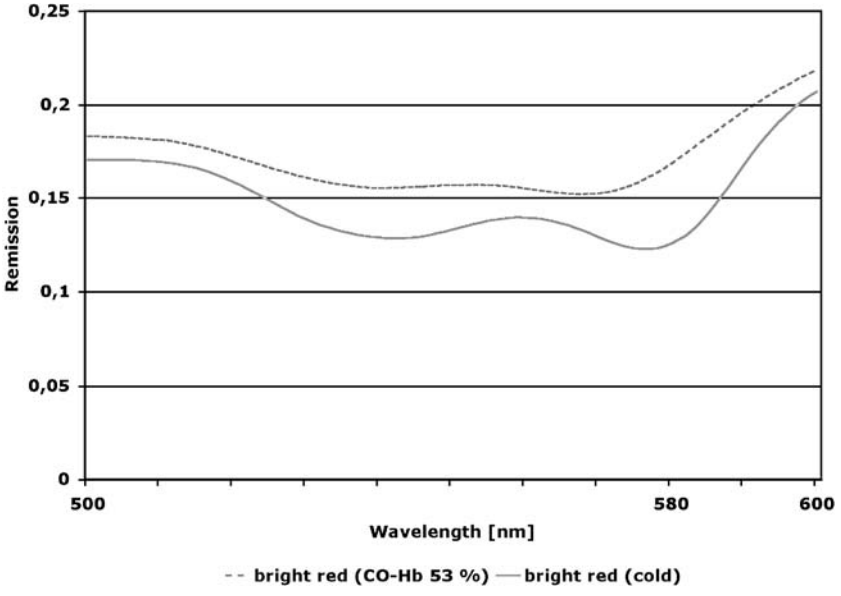

Fig. 3 Spectral reflectance curves of cherry red postmortem lividity in CO poisoning (*top curve*) and after exposure to low ambient temperatures (*bottom curve*) in the spectral range of 500–600 nm

sulfate was used as white standard according to DIN 5033. The measurements were controlled and evaluated with the help of a personal computer.

On each body, five separate measurements of postmortem lividity in the posterior lateral region of the thorax were performed, and the median was determined based on the spectral reflectance curves.

Estimation of carbon monoxide hemoglobin concentration

The Monte Carlo-based calibration model was estimated for a semi-infinite half space with a refractive index n_{cp} of 1.36 [13, 41, 55]. The reflectance $R_{r_c}(\mu_s, \mu_a, g)$ was calculated according to Eq. 1 for a detector radius r_c of 0.5 cm. The *effective* particle size distribution $h(d)$ of the scatterer (collagen fibers and mitochondria) was calculated from d=0.1 to 0.8 μm with a discretization Δd of 0.1 μm (Fig. 2). The extinction spectra of Hb, O_2-Hb, and CO-Hb and the skin pigments eumelanin and pheomelanin were taken into account for the modeling of the absorption coefficient. The desired parameters were estimated by a least squares fit of the measured reflectance spectrum in a range of 500 to 600 nm, in which the extinction spectrum of CO-Hb and O_2-Hb differ most (Fig. 3). The standard deviations were calculated under the assumption of the Gaussian error propagation.

Calibration of the Monte Carlo-based skin model and estimation of the CO-Hb concentrations were performed with a newly programmed software packet consisting of three programs, TMinv, TMinvReg, and BLT-TMinv, which are based on Tcl/Tk, using Linux Workstations. As described above, one simulation for a certain set of optical parameters required up to 3 h. The whole calibration consisting of up to 1,000 single simulations was performed parallely on different PCs and took about 7 days.

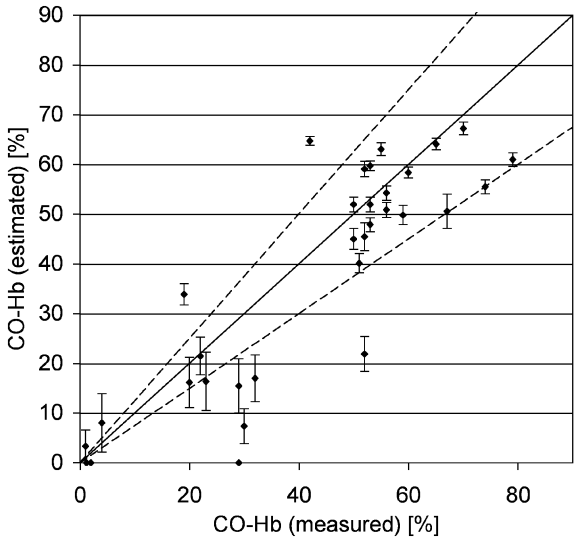

Fig. 4 Comparison of the CO-Hb values measured in the blood (*x axis*) and the CO-Hb values estimated by means of Monte Carlo simulations (±SD) in postmortem lividity. The *broken lines* mark the area of ±25% of the measured value

Table 1 Results of the CO-Hb measurements in heart blood (spectrophotometric analysis) and the CO-Hb estimations by the Monte Carlo-based skin model

No.	Measured CO-Hb (%)	Estimated CO-Hb±SD (%)
1	52	59±1.0
2	53	60±3.2
3	53	52±7.0
4	67	51±3.2
5	60	58±1.5
6	42	65±2.8
7	30	7±1.7
8	59	50±11.6
9	70	67±1.8
10	32	17±2.7
11	29	21±3.6
12	2	0±1.7
13	56	54±6.3
14	52	45±1.8
15	20	16±5.0
16	65	64±5.5
17	22	21±4.0
18	4	8±3.4
19	52	22±1.9
20	51	40±3.3
21	23	16±2.4
22	29	15±2.7
23	19	34±3.5
24	1	0±1.0
25	74	55±2.8
26	79	61±1.0
27	56	51±1.8
28	50	45±2.1
29	53	48±2.0
30	1	3±3.7
31	50	52±1.0
32	55	63±3.2

Standard deviations were calculated under the assumption of the Gaussian error propagation

Results

The estimations of the CO-Hb concentrations obtained with the Monte Carlo-based skin model and the actual values are indicated in Table 1. The values estimated with the help of the skin model tended to be lower than the actual values. With higher CO-Hb concentrations in the blood, the estimations were closer to the actual values, whereas with lower concentrations deviations of greater than 25% of the actual value were also seen (Fig. 4).

Discussion

In the past, spectral reflectance analyses on corpse skin were seldom performed mostly because of data processing

problems. Evaluating spectra over a whole spectral range involves a considerable amount of computational effort. For this reason, studies were often limited to isolated wavelengths, wherein characteristic changes could be observed. On the other hand, this limitation to isolated wavelengths leads both to a loss of information and to the reduction of the information on a whole spectrum to a few figures, as is the case with colorimetry [9]. More complex mathematical evaluation methods to analyze reflectance spectra have been used in legal medicine only in the more recent past, especially to classify the age of hematomas in living persons and to identify blood traces [28, 29, 43]. To evaluate the spectra, these studies used the method of k nearest neighbors and neuronal networks. Complex mathematical models were also developed for other purposes in legal medicine, such as the calculation of the cooling of a human body [36–38].

Characterization of a substance with the help of its optical properties is a customary analytical method, especially in chemistry and material research. Up to now, however, there is hardly any established optical method to identify or characterize a substance in the skin or to measure the concentration of an agent in the skin apart from a small number of specific procedures such as pulse oximetry. Only occasionally, the concentration of a substance in tissue was successfully determined by measuring the surface reflection, e.g., in the diagnosis of neonatal jaundice [3], for the determination of the glucose concentration in the blood [17], the content of hemoglobin in skin vessels [56], or the oxygen partial pressure in the tissue [14, 16, 18, 30, 39]. In contrast to many other methods, the Monte Carlo-based model proposed in this article was developed not only for classification, but also for quantitative estimation of the respective biomedical parameter, i.e., the CO saturation of hemoglobin.

Analysis and quantification of hemoglobin and its variants can gain great importance in medicolegal casework [8, 23], especially in fire victims where the detection of carbon monoxide hemoglobin is crucial for the diagnoses of the cause of death and the vitality [12].

Determination of the CO-Hb concentration in corpse blood is one of the routine tests in forensic toxicology, for which proven methods (spectrophotometry, GC/MS) were established long ago. From a toxicological viewpoint, there is no need to develop a new technique. The purpose of this study was not to establish another analytical method but to validate the Monte Carlo-based skin model presented. Although this model is a preliminary one, a good correlation between the estimated values and the values measured in the corpse blood by means of spectrophotometry was achieved in general. Considering the great similarity of the extinction spectra of CO-Hb and O_2-Hb [47], this correlation is remarkable. With the Monte Carlo-based model we were able to decide clearly on the basis of the investigated reflectance spectra whether the pink color of livor mortis was due to the content of CO-Hb or of O_2-Hb. In contrast to the model-free analysis [9], this was possible not only in CO-Hb concentrations exceeding 50%. Furthermore, it was possible to calculate the CO-Hb concentration in the blood in the postmortem lividity, although with some minor variations to the actual values measured in the corpse blood.

The deviations between the estimated and the actual values may be attributable both to inaccuracies in the model and to individual differences in the study material (skin pigmentation, intensity of hypostasis depending on blood content in the vessels). A further adjustment of the model is necessary. The problem is how to validate the model parameters, which are difficult or even impossible to determine by means of an alternative measuring method in the individual case. For example, the concentration of melanin in the investigated skin area cannot be measured objectively. In addition, it has to be taken into account that the scattering and absorption behavior of the skin may be different due to postmortem changes (shift of fluid in the tissue, autolysis, and putrefaction). Up to now the skin model is based on parameters referring to human skin in vivo. The next question to be investigated is how the optical behavior of the skin changes postmortem. Meanwhile an application has been filed with the German Patent and Trademark Office for the method to determine the optical properties of optically turbid media by means of integral reflectance spectroscopy.

Acknowledgements This study was supported by Deutsche Forschungsgemeinschaft (German Research Council), file number BO 1923/2-1.

References

1. Anderson RR, Parrish JA (1981) The optics of human skin. J Invest Dermatol 77:13–19
2. Aronson R, Corngold N (1999) Photon diffusion coefficient in an absorbing medium. J Opt Soc Am A 16:1066–1071
3. Ballowitz L, Avery ME (1970) Spectral reflectance of the skin. Biol Neonate 15:348–360
4. Blazek V, Wehr K (1976) Ein Verfahren zur eindeutigen optischen Klassifizierung von menschlicher Haut. Beitr Gerichtl Med 34:161–171
5. Blazek V (1977) Forensische Anwendungen der spektralen Remissionsanalyse menschlicher Haut mit einer beweglichen photometrischen Kugel. Z Rechtsmed 79:47–62
6. Blazek V (1979) Ein optoelektronisches Meßverfahren zur farbvalenzmetrischen Bewertung der menschlichen Haut. Thesis, RWTH, Aachen
7. Blazek V (1980) Deutung ausgewählter, forensisch relevanter Veränderungen der wellenlängenabhängigen Hautreflexion. Biomed Tech 25:417–419
8. Bock H, Seidl S, Hausmann R, Betz P (2004) Sudden death due to a haemoglobin variant. Int J Legal Med 118:95–97
9. Bohnert M, Weinmann W, Pollak S (1999) Spectrophotometric evaluation of postmortem lividity. Forensic Sci Int 99:149–158
10. Bohnert M, Baumgartner R, Pollak S (2000) Spectrophotometric evaluation of the colour of intra- and subcutaneous bruises. Int J Legal Med 113:343–348
11. Bohnert M (2001) Bedeutung und Einsatzmöglichkeiten optischer Verfahren in der Rechtsmedizin. Habilitationsschrift, University of Freiburg
12. Bohnert M, Werner CR, Pollak S (2003) Problems associated with the diagnosis of vitality in burned bodies. Forensic Sci Int 135:197–205
13. Bolin FP, Preuss LE, Taylor CR, Ference RJ (1989) Refractive index of some mammalian tissues using a fibre optic cladding method. Appl Opt 28:2297–2303

14. Caspary L, Thum J, Creutzig A, Lübbers DW, Alexander K (1995) Quantitative reflection spectrophotometry: spatial and temporal variation of Hb oxygenation in human skin. Int J Microcirc Clin Exp 15:131–136
15. Deutsche Forschungsgemeinschaft (1988) Photometrische Bestimmung von Carboxy-Hämoglobin (CO-Hb) im Blut. VCH, Weinheim
16. Feather JW, Ellis DJ, Leslie G (1988) A portable reflectometer for the rapid quantification of cutaneous haemoglobin and melanin. Phys Med Biol 33:711–722
17. Fischbacher C (1997) Untersuchungen und chemometrische Strategien zur nichtinvasiven Bestimmung der Blutglucose mittels Nahinfrarot-Reflexionsspektroskopie. Thesis, Friedrich-Schiller-Universität, Jena
18. Frank KH, Kessler M, Appelbaum K, Dümmler W (1989) The Erlangen micro-lightguide spectrophotometer EMPHO I. Phys Med Biol 34:1883–1900
19. Hendricks JS, Booth TE (1985) MCNP variance reduction overview. Lect Notes Phys 240:83–92
20. Honerkamp J, Weese J (1990) Tikhonov's regularization method for ill-posed problems: a comparison of different methods. Contin Mech Thermodyn 2:17–30
21. Inoue H, Suyama A, Matuoka T, Inoue T, Okada K, Irizawa Y (1994) Development of an instrument to measure postmortem lividity and its preliminary application to estimate the time since death. Forensic Sci Int 65:185–193
22. Ishimura A (1997) Light scattering in turbid media. IEEE Press, New York
23. Iwersen-Bergmann S, Schmoldt A (2000) Acute intoxication with aniline: detection of acetaminophen as aniline metabolite. Int J Legal Med 113:171–174
24. Kaatsch HJ, Stadler M, Nietert M (1993) Photometric measurement of color changes in livor mortis as a function of pressure and time. Int J Legal Med 106:91–97
25. Kaatsch HJ, Schmidtke W, Nietsch W (1994) Photometric measurement of pressure-induced blanching of livor mortis as an aid to estimating time of death. Int J Legal Med 106:91–97
26. Keijzer M, Jacques SL, Prahl SA, Welch AJ (1989) Light distributions in artery tissue: Monte Carlo simulations for finite-diameter laser beams. Lasers Surg Med 9:148–154
27. Kienle A, Patterson MS (1996) Determination of the optical properties of turbid media from a single Monte Carlo simulation. Phys Med Biol 41:2221–2227
28. Klein A, Schweitzer D, Schote I, Wolf C (1992) Spektrometrie zur Hämatomaltersbestimmung beim Lebenden. Beitr Gerichtl Med 50:235–240
29. Klein A, Rommeiß S, Fischbacher C, Jagemann K-U, Danzer K (1996) Estimating the age of hematomas in living subjects based on spectrometric measurements. In: Oehmichen M, Kirchner H (eds) The wound healing process: forensic pathological aspects. Schmidt-Römhild, Lübeck, pp 283–291
30. Kuchenreuter S, Adler J, Schütz W, Eichelbrönner O, Georgieff M (1996) The Erlanger microlightguide photometer: a new concept for monitoring intracapillary oxygen supply of tissue—first results and a review of the physiological basis. J Clin Monit 12:211–224
31. Lins G (1968) Die Remissionsanalyse zur farblichen Charakterisierung der Leichenhaut. Beitr Gerichtl Med 24:162–166
32. Lins G (1973) Der Farbort der Totenflecken im Spektralfarbenzug. Beitr Gerichtl Med 31:203–212
33. Lins G, Kutschera J (1974) Die farbmetrische Bewertung der Grünfäule der Leichenhaut im Rahmen der programmierten Farbwertintegration. Z Rechtsmed 75:201–212
34. Lins G (1975) Die farbanalytische Bewertung forensisch relevanter Hautveränderungen. Theoretische und praktische Grundlagen am Menschen. Habilitationsschrift, University of Frankfurt
35. Lins G, Blazek V (1982) Die Anwendung der Remissionsanalyse zur direkten farbmetrischen Bestimmung des Blutfleckenalters. Z Rechtsmed 88:13–22
36. Mall G, Hubig M, Beier G, Eisenmenger W (1998) Energy loss due to radiation in postmortem cooling. Part A: quantitative estimation of radiation using the Stefan–Boltzmann law. Int J Legal Med 111:299–304
37. Mall G, Hubig M, Beier G, Büttner A, Eisenmenger W (1999) Energy loss due to radiation in postmortem cooling. Part B: energy balance with respect to radiation. Int J Legal Med 112: 233–240
38. Mall G, Eckl M, Sinicina I, Peschel O, Hubig M (2004) Temperature-based death time estimation with only partially known environmental conditions. Int J Legal Med, published online
39. Merschbrock U, Hoffmann J, Caspary L, Huber J, Schmickaly U, Lübbers DW (1994) Fast wavelength scanning reflectance spectrophotometer for noninvasive determination of hemoglobin oxygenation in human skin. Int J Microcirc 14:274–281
40. Oregon Medical Laser Center (2001) Optical properties spectra. http://omlc.ogi.edu/spectra/
41. Perelman LT, Backman V, Wallace M, Zonios G, Manoharan R, Nusrat A, Shields S, Seiler M, Lima C, Hamano T, Itzkan I, Dam JV, Crawford JM, Feld MS (1998) Observation of periodic fine structure in reflectance from biological tissue: a new technique for measuring nuclear size distribution. Phys Rev Lett 80:627–630
42. Press WH, Teukolsky SA, Vetterling WT, Flanner BP (2002) Numerical recipes in C++. Cambridge University Press, New York
43. Rommeiß S, Ruppe S, Fischbacher C, Jagemann KU, Klein A (2000) Zerstörungsfreier Blutnachweis in blutverdächtigen Spuren mittels VIS-Spektrometrie. In: Rothschild MA (ed) Das neue Jahrtausend: Herausforderungen an die Rechtsmedizin. Schmidt-Römhild, Lübeck, pp 377–384
44. Schaefer AT (2000) Colour measurements of pallor mortis. Int J Legal Med 113:81–83
45. Schuller E, Pankratz H, Liebhardt E (1987) Farbortmessungen an Totenflecken. Beitr Gerichtl Med 45:169–173
46. Schuller E, Pankratz H, Wohlrab S, Liebhardt E (1988) Die Bestimmung des Farbortes der Totenflecken in Beziehung zur Wegdrückbarkeit. In: Bauer G (ed) Gerichtsmedizin. Festschrift für W. Holczabek. Franz Deuticke, Wien, pp 295–302
47. Schwerd W (1962) Der rote Blutfarbstoff und seine wichtigsten Derivate. Schmidt-Römhild, Lübeck
48. Thornton JI (1997) Visual color comparison in forensic science. Forensic Sci Rev 9:37–56
49. Tikhonov AN, Arsenin VY (1977) Solutions of ill-posed problems. Wiley, New York
50. van de Hulst HC (1980) Multiple light scattering. Academic, New York
51. Vanezis P (1991) Assessing hypostasis by colorimetry. Forensic Sci Int 52:1–3
52. Vanezis P, Trujillo O (1996) Evaluation of hypostasis using a colorimeter measuring system and its application to assessment of the post-mortem interval (time of death). Forensic Sci Int 78:19–28
53. Walther R, Roths T, Bohnert M, Honerkamp J (2004) Monte Carlo based model for steady-state diffuse reflectance spectroscopy. Proc SPIE 5261:70–81
54. Wang L, Jacques SL (1992) Monte Carlo modeling of light transport in multi-layered tissues in standard C. Anderson Cancer Center, University of Texas, Houston
55. Zonios G, Perelman LT, Backman V, Manoharan R, Fitzmaurice M, Dam JV, Feld MS (1999) Diffuse reflectance spectroscopy of human adenomatous colon polyps in vivo. Appl Opt 38:6628–6637
56. Zonios G, Bykowski J, Kollias N (2001) Skin melanin, hemoglobin, and light scattering properties can be quantitatively assessed in vivo using diffuse reflectance spectroscopy. J Invest Dermatol 117:1452–1457